

Mixed properties of magnetohydrodynamic waves undergoing resonant absorption in the cusp continuum

M. Goossens¹, S.-X. Chen², M. Geeraerts¹, B. Li², and T. Van Doorselaere¹

¹ Centre for mathematical Plasma Astrophysics (CmPA), KU Leuven, Celestijnenlaan 200B bus 2400, B-3001 Leuven, Belgium

² Shandong Provincial Key Laboratory of Optical Astronomy and Solar-Terrestrial Environment, Institute of Space Sciences, Shandong University, Weihai 264209, People's Republic of China

ABSTRACT

Context. Observations of magnetohydrodynamic (MHD) waves in the structured solar atmosphere have shown that these waves are damped and can thus contribute to atmospheric heating. In this paper, we focus on the damping mechanism of resonant absorption in the cusp continuum. This process takes place when waves travel through an inhomogeneous plasma.

Aims. Our aim is to determine the properties of MHD waves undergoing resonant absorption in the cusp continuum in the transition layer of a cylindrical solar atmospheric structure, such as a photospheric pore or a coronal loop. Depending on which quantities dominate, one can assess what type of classical MHD wave the modes in question resemble most.

Methods. In order to study the properties of these waves, we analytically determine the spatial profiles of compression, displacement, and vorticity for waves with frequencies in the cusp continuum, which undergo resonant absorption. We confirm these analytical derivations via numerical calculations of the profiles in the resistive MHD framework.

Results. We show that the dominant quantities for the modes in the cusp continuum are the displacement parallel to the background magnetic field and the vorticity component in the azimuthal direction (i.e. perpendicular to the background magnetic field and along the loop boundary).

Key words. magnetohydrodynamics (MHD) – waves – Sun: corona – Sun: magnetic fields

1. Introduction

In non-uniform plasmas, magnetohydrodynamic (MHD) waves behave differently than their counterparts in uniform plasmas of infinite extent (Goossens et al. 2019). In the latter case, the MHD waves can be separated into Alfvén waves and magnetosonic waves. The situation is different in a non-uniform plasma. The clear division between Alfvén waves and magnetosonic waves is no longer present. The MHD waves have mixed properties. The general rule is that MHD waves propagate both parallel vorticity, as in classic Alfvén waves, and compression, as in classic magnetosonic waves. The present paper is a companion to the paper by Goossens et al. (2020), which dealt with resonant damping in the Alfvén continuum. In that paper, plasma pressure was neglected but here it plays an essential role. Goossens et al. (2020) focused on the properties of MHD waves that undergo resonant absorption in the Alfvén continuum. They considered a straight magnetic field and in addition assumed that the plasma is pressureless. This assumption removes the slow magnetosonic part of the spectrum as well as the resonant absorption in the cusp continuum. Since the focus here will be on the behaviour in the cusp continuum, we include plasma pressure in the analysis.

Interest in the resonant behaviour of MHD waves has mainly been concentrated on resonant absorption in the Alfvén continuum (Goossens et al. 1992, 2002; Soler et al. 2013). Recently, there has been increased interest in the cusp continuum because of the observation of MHD waves in the lower solar atmosphere. These waves have been observed in the chromosphere (De Pontieu et al. 2007; Morton et al. 2012; Verth & Jess

2016) as well as in the photosphere (Dorotovič et al. 2008; Fujimura & Tsuneta 2009; Grant et al. 2015; Moreels et al. 2015; Keys et al. 2018; Gilchrist-Millar et al. 2020). The oscillations observed in a photospheric magnetic pore by, for example, Grant et al. (2015) display characteristics of rapidly decaying slow surface sausage modes (SSSMs). Yu et al. (2017) analytically calculated the damping rate of these modes by resonant absorption in the slow continuum in the thin boundary limit. In a numerical study, Chen et al. (2018) compared the damping rates of SSSMs due to resonant absorption in the slow continuum with the damping rate due to Ohmic resistivity. Their numerical results were later confirmed by the analytical derivations in Geeraerts et al. (2020). In another numerical study, Chen et al. (2020) compared the damping rates of slow surface kink modes (SSKMs) due to resonant absorption in the Alfvén and slow continua with the damping rate due to Ohmic resistivity.

In the present investigation, we focus on the eigenvalue problem (EVP) and try to understand what happens when the wave is actually damped in non-stationary MHD. We take the frequency to be complex and relate the spatial behaviour to the damping properties of the MHD wave. The temporal and spatial variation of the perturbed quantities is therefore described by the factor

$$\exp\{i(m\varphi + k_z z - \omega t)\}.$$

Here, m and k_z are, respectively, the azimuthal and longitudinal wave numbers, and ω is the complex frequency with

$$\omega = \omega_R + i\omega_I, \quad \omega_I = \gamma.$$

Since we focus on the EVP, we do not have to worry about possible Gaussian damping that can occur in the temporal evolution after the initial excitation. This Gaussian damping is well known for propagating (Pascoe et al. 2010, 2011, 2012; Hood et al. 2013) and standing kink waves (Ruderman & Terradas 2013; Guo et al. 2020) in coronal loops. However, it is not clear to us whether this behaviour has been observed, in real life or in numerical experiments, regarding the temporal evolution for slow waves in the photosphere.

Studies on resonant absorption have mainly focused on the components of the displacement, the amount of absorbed energy, and the damping rate. Little to no attention has been paid to the change in the spatial behaviour of fundamental quantities such as compression and vorticity. Analytical solutions for the components of the Lagrangian displacement in the dissipative layer have been derived by, for example, Sakurai et al. (1991) and Goossens et al. (1995) for resonant MHD waves in ideal and dissipative stationary MHD.

Resonant absorption has a long history in fusion plasma physics, space plasma physics, solar physics, and astrophysics. A characterization was given by Parker (1991), who noted that resonant absorption in the Alfvén continuum is to be expected when a wave with a phase velocity ω/k spans a region in which the variation of the Alfvén velocity v_A across the region provides the resonance condition $\omega/k = v_A$. Non-uniformity is key to the process. The Alfvén velocity v_A and the Alfvén frequency ω_A depend on position. The resonance occurs at the position r_A where the frequency of the wave ω is equal to the local Alfvén frequency, $\omega = \omega_A(r_A)$.

Resonant absorption has been studied extensively for frequencies in the Alfvén continuum. For example, since 2002 (Ruderman & Roberts 2002; Goossens et al. 2002), resonant absorption of kink waves has been a popular mechanism for explaining the rapid damping of standing and propagating MHD waves in coronal loops. The simple model invokes MHD waves superimposed on a cylindrical plasma column in static equilibrium. Cylindrical coordinates (r, φ, z) are used. The inhomogeneity necessary for resonant absorption to operate is usually provided by the equilibrium density $\rho_0(r)$, which varies from ρ_i to ρ_e in the interval $[R - l/2, R + l/2]$. The density ρ_0 is constant in the internal and external parts of the loop with values ρ_i and ρ_e .

Relatively simple analytic expressions for the ratio of the damping time over the period for standing MHD waves can be obtained by using the thin tube and thin boundary (TTTB) approximation. The TTTB approximation means that $k_z R \ll 1$ and $l/R \ll 1$. Analytical expressions for the damping time τ_D were derived by Hollweg (1990), Goossens et al. (1995), Ruderman & Roberts (2002), Van Doorselaere et al. (2004), and Arregui & Goossens (2019). The expression given by Arregui & Goossens (2019) is

$$\frac{\tau_D}{\text{Period}} = \frac{1}{|m|} \frac{4}{\pi^2} \frac{\alpha}{l/R} \frac{\rho_i + \rho_e}{\rho_i - \rho_e}, \quad (1)$$

where period = $2\pi/\omega_R$, γ is the damping decrement, and $\tau_d = 1/|\gamma|$ is the damping time. The variation of density is confined to a layer of thickness l and has steepness α .

Resonant absorption in the cusp continuum has already been studied in previous works, such as Keppens (1995), Soler et al. (2009), Yu et al. (2017), Chen et al. (2018), and Yu & Van Doorselaere (2019). For a straight field, there is no resonant damping of axisymmetric modes in the Alfvén continuum (Sakurai et al. 1991). Resonant damping in the cusp con-

tinuum occurs for axisymmetric ($m = 0$) and non-axisymmetric motions if their frequency is in the cusp continuum. In this process, the wave excites local oscillations with the same frequency and with properties close to those of the slow waves from an infinite homogeneous plasma, as will be discussed in this paper. An analytical expression for the ratio of the damping time over the period is rather involved for axisymmetric motions and has been derived in Yu et al. (2017). An expression for non-axisymmetric motions can be found in Soler et al. (2009), where they compare the efficiency of the damping of the kink mode by resonant absorption in the cusp continuum with the resonant absorption in the Alfvén continuum. Chen et al. (2018) compare the damping of SSSMs in photospheric pore conditions by resonant absorption with that by electrical resistivity.

As explained, for example, in Goossens et al. (2019), whether MHD waves in a given inhomogeneous plasma have Alfvénic, fast, or slow magnetosonic properties can be assessed by looking at the displacement components, as well as the compression and the vorticity carried by these waves. In this paper, our interest therefore lies in deriving the spatial profiles of the compression as well as the displacement and vorticity components of MHD waves with frequencies in the cusp continuum.

2. MHD waves with mixed properties for a straight field

The mixed properties of the MHD waves in an inhomogeneous plasma arise because the equations that rule them are coupled. This was pointed out by, for example, Goossens et al. (2019), who showed that the waves have features of both Alfvén waves (namely a non-zero parallel vorticity) and magnetosonic waves (non-zero compression). The coupling of the MHD equations is controlled by the coupling functions C_A and C_S , which were first introduced by Sakurai et al. (1991). For a straight field, $\mathbf{B}_0 = B_z(r)\mathbf{1}_z$, these two constants take the simple form

$$C_A = g_B P' = \frac{m}{r} B_z P', \quad C_S = P'. \quad (2)$$

This means that the equations are coupled because of P' . The importance of P' for resonant absorption has been discussed by, for example, Hasegawa & Uberoi (1982), Hollweg & Yang (1988), Tirry & Goossens (1995), and Soler et al. (2013).

Since we are dealing with non-stationary MHD waves, the frequency ω is a complex quantity with an imaginary part expressing the damping rate. Goossens et al. (2020) studied the behaviour of MHD waves that undergo resonant absorption in the Alfvén continuum. They considered a pressureless plasma, which helps to simplify the analysis and is often a good approximation of reality for the Alfvén resonance. The situation for the slow resonance is different, however. First of all, plasma pressure is essential because there are no slow waves in a pressureless plasma. Secondly, there is resonant absorption in the cusp continuum for axisymmetric waves ($m = 0$) in the same way as for non-axisymmetric waves.

The expressions for the components of the displacement ξ and compression can be found, for example, in Goossens et al. (2019) (see equation (45) therein):

$$\begin{aligned}
\xi_r &= \frac{1}{\rho_0(\omega^2 - \omega_A^2)} \frac{dP'}{dr}, \\
\xi_\perp &= \xi_\varphi = \frac{im/r}{\rho_0(\omega^2 - \omega_A^2)} P', \\
\xi_\parallel &= \xi_z = ik_z \frac{v_s^2}{v_s^2 + v_A^2} \frac{1}{\rho_0(\omega^2 - \omega_C^2)} P', \\
\nabla \cdot \xi &= \frac{-\omega^2}{(v_s^2 + v_A^2)} \frac{1}{\rho_0(\omega^2 - \omega_C^2)} P'. \quad (3)
\end{aligned}$$

The quantities ω_A and ω_C are the local Alfvén frequency and the local cusp frequency, respectively. They are defined as

$$\begin{aligned}
\omega_A^2 &= \frac{(\mathbf{k} \cdot \mathbf{B})^2}{\mu\rho} = k_z^2 v_A^2 = k_\parallel v_A^2, \\
\omega_C^2 &= \frac{v_s^2}{v_s^2 + v_A^2} \omega_A^2 = \frac{v_s^2}{v_s^2 + v_A^2} k_z^2 v_A^2 = k_z^2 v_C^2, \quad (4)
\end{aligned}$$

where v_A , v_s , and v_C are the Alfvén speed, sound speed, and cusp speed, respectively. They are defined as

$$v_A^2 = \frac{B_0^2}{\mu\rho_0}, \quad v_s^2 = \frac{\gamma p_0}{\rho_0}, \quad v_C^2 = \frac{v_A^2 v_s^2}{v_A^2 + v_s^2}, \quad (5)$$

with $\gamma = c_p/c_v$ the ratio of the specific heats and p_0 the equilibrium thermal pressure. This should not be confused with the temporal decrement in equation (1). In a non-uniform plasma, the characteristic frequencies ω_A and ω_C depend on position and define the Alfvén and cusp continua.

Similarly, equation (53) from Goossens et al. (2019) gives the expressions for the components of $\nabla \times \xi$:

$$\begin{aligned}
(\nabla \times \xi)_r &= k_z \frac{m}{r} \frac{v_A^2}{v_s^2 + v_A^2} \frac{\omega^2}{\rho_0(\omega^2 - \omega_A^2)(\omega^2 - \omega_C^2)} P', \\
(\nabla \times \xi)_\varphi &= (\nabla \times \xi)_\perp \\
&= ik_z \frac{1}{\{\rho_0(\omega^2 - \omega_C^2)\}^2} \frac{d}{dr} \left\{ \rho_0(\omega^2 - \omega_C^2) \right\} \frac{v_s^2}{v_A^2 + v_s^2} P' \\
&\quad + ik_z \frac{\omega^2}{\rho_0(\omega^2 - \omega_A^2)(\omega^2 - \omega_C^2)} \frac{v_A^2}{v_A^2 + v_s^2} \frac{dP'}{dr} \\
(\nabla \times \xi)_z &= (\nabla \times \xi)_\parallel \\
&= -i \frac{m}{r} \frac{1}{\{\rho_0(\omega^2 - \omega_A^2)\}^2} \frac{d}{dr} \left\{ \rho_0(\omega^2 - \omega_A^2) \right\} P'. \quad (6)
\end{aligned}$$

Equations (3) and (6) clearly show that P' plays the role of a coupling function. The horizontal components of vorticity $(\nabla \times \xi)_r$ and $(\nabla \times \xi)_\varphi$ are always non-zero, whereas the parallel vorticity $(\nabla \times \xi)_z$ is only non-zero if

$$\frac{d}{dr} \left\{ \rho_0(\omega^2 - \omega_A^2) \right\} \neq 0, \quad (7)$$

that is to say, in the inhomogeneous transition layer (TL) at the loop boundary (where the density varies with r). In

a non-uniform plasma, all the quantities are non-zero. As a consequence, the MHD waves are neither pure Alfvén waves (which have zero compression) nor pure magnetosonic waves (which have zero parallel vorticity). As was pointed out by Goossens et al. (2002, 2006, 2008, 2011, 2012, 2019), MHD waves in a non-uniform plasma have mixed properties that change as the waves travel through the inhomogeneous part of the plasma.

Goossens et al. (2020) focused on MHD waves that undergo damping in the Alfvén continuum. They showed that $(\nabla \times \xi)_\parallel$ is much larger than $(\nabla \times \xi)_r$ and $(\nabla \times \xi)_\varphi$ in the inhomogeneous TL. Since in a homogeneous plasma of infinite extent only Alfvén waves propagate parallel vorticity, this showed that waves undergoing resonant absorption in the Alfvén continuum are very close to Alfvén waves in their nature despite having non-zero compression.

Here we study MHD waves that undergo damping by resonant absorption in the cusp continuum. In what follows, we show that, contrary to the Alfvén continuum, the parallel component of vorticity does not play any significant role here. Instead, we will show that the perpendicular component of the vorticity, $(\nabla \times \xi)_\varphi$, is dominant. In particular, the first term on the right-hand side of $(\nabla \times \xi)_\perp$ will be important. This term is non-zero when

$$\frac{d}{dr} \left\{ \rho_0(\omega^2 - \omega_C^2) \right\} \neq 0. \quad (8)$$

In the particular case of a constant straight field, $\mathbf{B}_0 = B_0 \mathbf{1}_z$, the equation of motion demands that the thermal pressure p_0 also be constant. We then have the simplifying relations

$$\begin{aligned}
\rho_0 v_A^2 &= \frac{B_0^2}{\mu_0} = \text{constant}, \quad \rho_0 \omega_A^2 = k_z^2 \frac{B_0^2}{\mu_0} = \text{constant}, \\
\frac{v_s^2}{v_A^2 + v_s^2} &= \text{constant}, \quad \rho_0 \omega_C^2 = \rho_0 \frac{v_s^2}{v_A^2 + v_s^2} \omega_A^2 = \text{constant}, \quad (9)
\end{aligned}$$

and the spatial variation of ω_A^2 and ω_C^2 is then solely due to the spatial variation of the equilibrium density ρ_0 . Hence,

$$\frac{d\rho_0}{dr} \neq 0 \quad (10)$$

is the important quantity for the resonant behaviour both in the Alfvén continuum and in the cusp continuum in case of a constant background magnetic field. For the cusp continuum, we also need $v_s^2 \neq 0$. We note that we will not use the simplifying assumption that the straight magnetic field $B_0 \mathbf{1}_z$ is constant because p_0 and B_0 are not constant in pores. The simplifications in Eq. (9) are thus not used in what follows.

The expression for the parallel component of vorticity under this assumption was given by equation (11) in Goossens et al. (2020):

$$\begin{aligned}
(\nabla \times \xi)_\parallel &= (\nabla \times \xi)_z \\
&= -i \frac{m}{r} \frac{\omega^2}{\{\rho_0(\omega^2 - \omega_A^2)\}^2} \frac{d\rho_0}{dr} P'. \quad (11)
\end{aligned}$$

The perpendicular component can similarly be calculated by noting, using Eq. (9), that

$$\frac{d}{dr} \{ \rho_0 (\omega^2 - \omega_C^2) \} = \omega^2 \frac{d\rho_0}{dr}$$

to find that

$$\begin{aligned} (\nabla \times \xi)_\perp &= (\nabla \times \xi)_\varphi \\ &= ik_z \frac{v_s^2}{v_s^2 + v_A^2} \frac{\omega^2}{\{ \rho_0 (\omega^2 - \omega_C^2) \}^2} \frac{d\rho_0}{dr} P' \\ &+ ik_z \frac{\omega^2}{(\omega^2 - \omega_A^2)} \frac{v_A^2}{v_A^2 + v_s^2} \frac{1}{\rho_0 (\omega^2 - \omega_C^2)} \frac{dP'}{dr}. \end{aligned} \quad (12)$$

The first term on the right-hand side of $(\nabla \times \xi)_\varphi$ is the dominant term for frequencies in the cusp continuum, as we shall explain in the next section. It is remarkably similar to Eq. (11).

We recall from Eq. (3) that P' is related to $\nabla \cdot \xi$ by an algebraic equation. Hence, it is straightforward to express $(\nabla \times \xi)_\parallel$ and $(\nabla \times \xi)_\perp$ in terms of $\nabla \cdot \xi$, so that parallel and perpendicular vorticity go together with compression in a non-uniform plasma.

3. Analysis of slow resonant waves close to the resonant point

We now consider a standing MHD wave that is damped by undergoing resonant absorption in the cusp continuum. Therefore, the longitudinal wavenumber k_z is real and the frequency is complex:

$$\omega = \omega_R + i\gamma, \quad \gamma = \omega_I, \quad \omega_R = \omega_C(r_C). \quad (13)$$

The frequency ω_R and the damping decrement γ are related to the period and the damping time as

$$\begin{aligned} \frac{1}{|\gamma|} &= \tau_D, \quad \text{Period} = \frac{2\pi}{\omega_R}, \\ \frac{\tau_D}{\text{Period}} &= \frac{1/|\gamma|}{2\pi/\omega_R} = \frac{1}{2\pi} \frac{\omega_R}{|\gamma|}, \\ \frac{|\gamma|}{\omega_R} &= \frac{1}{2\pi} \frac{\text{Period}}{\tau_D}. \end{aligned} \quad (14)$$

In view of the periods and damping times observed in waves in the solar corona, it is a good approximation to assume

$$\frac{|\gamma|}{\omega_R} \ll 1, \quad (15)$$

which represents weak damping. The focus goes to the position r_C , where the ideal resonance occurs: $\omega^2 = \omega_C^2(r_C)$. The comments in Goossens et al. (2020) about the position where the resonance occurs, explaining that it is actually off the real axis, apply here as well. As explained there, the assumption of non-stationary MHD (namely that ω is complex) entails that the resonant position r_C will be complex as well. In the case of a weak damping, as expressed by Eq. (15), the imaginary part of r_C will also be small compared to its real part, and we can make the approximation to neglect it and consider r_C to be real.

The results that are discussed in this section actually describe the MHD waves just outside the infinitely thin resonant layer. The waves inside this layer are not addressed, as resistive effects

become too important to be ignored there, so that ideal MHD is not a valid approximation. However, barring the resonant layer, the ideal MHD solutions are a good approximation of the full resistive solution for sufficiently small damping, and therefore the results from the ideal MHD calculations that are made here make physical sense.

In what follows, we simplify the expressions for the wave variables by retaining only the dominant terms in $|\gamma|/\omega_R$. The dominant contributions to $\xi_\parallel = \xi_z$, $\nabla \cdot \xi$, $(\nabla \times \xi)_r$, and $(\nabla \times \xi)_\varphi$ are caused by the terms

$$\frac{1}{\rho_0 (\omega^2 - \omega_C^2)} \quad \text{and} \quad \frac{1}{\{ \rho_0 (\omega^2 - \omega_C^2) \}^2},$$

which lead, respectively, to behaviour proportional to

$$\frac{\tau_D}{\text{Period}} \quad \text{and} \quad \left\{ \frac{\tau_D}{\text{Period}} \right\}^2,$$

as we will derive next. The quantities ξ_r , $\xi_\perp = \xi_\varphi$, and $(\nabla \times \xi)_z$ do not have a factor of the form

$$\frac{1}{\{ \rho_0 (\omega^2 - \omega_C^2) \}^n}, \quad n \geq 1 \quad (16)$$

and are therefore independent of τ_D/Period . These quantities do not feel the cusp resonance and thus do not play an important role in the process of resonant absorption in the cusp continuum.

We will first consider the parallel component of displacement $\xi_z = \xi_\parallel$ and compression $\nabla \cdot \xi$. These two quantities are proportional to Eq. (16) with $n = 1$. We use the following intermediate results for weak damping:

$$\begin{aligned} \omega^2 &= (\omega_R + i\gamma)^2 \approx \omega_R^2 + 2i\gamma\omega_R, \\ \rho_0 (\omega^2 - \omega_C^2) &\approx 2i\rho_0(r_C)\omega_R^2 \frac{\gamma}{\omega_R}, \\ \frac{1}{\rho_0 (\omega^2 - \omega_C^2)} &\approx -i \frac{\pi}{\rho_0(r_C)\omega_R^2} \frac{\tau_D}{\text{Period}}. \end{aligned} \quad (17)$$

We then find the following approximations for parallel displacement and compression:

$$\begin{aligned} \xi_z &\approx k_z \frac{v_s^2}{v_s^2 + v_A^2} \frac{\pi}{\rho_0 \omega_R^2} \frac{\tau_D}{\text{Period}} P', \\ \nabla \cdot \xi &\approx -i \frac{\pi}{\rho_0 (v_s^2 + v_A^2)} \frac{\tau_D}{\text{Period}} P'. \end{aligned} \quad (18)$$

We will now consider the radial component of vorticity $(\nabla \times \xi)_r$ in Eq. (6). Like ξ_z and $\nabla \cdot \xi$, this quantity is proportional to Eq. (16) with $n = 1$. In addition, there is a factor $1/(\omega^2 - \omega_A^2)$. Since

$$\omega^2 - \omega_A^2 \approx \omega_C^2 - \omega_A^2 \approx -\frac{v_A^2}{v_s^2} \omega_R^2, \quad (19)$$

it follows that

$$(\nabla \times \xi)_r \approx -i \pi k_z \frac{m}{r} \frac{v_s^2}{v_s^2 + v_A^2} \frac{1}{\rho_0 \omega_R^2} \frac{\tau_D}{\text{Period}} P'. \quad (20)$$

We now turn to the perpendicular component of vorticity, $(\nabla \times \xi)_\phi$. The first term in its expression from Eq. (6) is the dominant term since it contains the factor Eq. (16) with $n = 2$. We thus discard the second term and find, from Eq. (17), that the dominant factor is approximated by

$$\frac{1}{\{\rho_0(\omega^2 - \omega_C^2)\}^2} \approx -\frac{\pi^2}{\rho_0^2 \omega_R^4} \left\{ \frac{\tau_D}{\text{Period}} \right\}^2,$$

while for the factor with the derivative we have

$$\begin{aligned} \frac{d}{dr} \{\rho_0(\omega^2 - \omega_C^2)\} &= \frac{d\rho_0}{dr} (\omega^2 - \omega_C^2) - \rho_0 k_z^2 \frac{dv_C^2}{dr} \\ &\approx \frac{d\rho_0}{dr} \frac{i\omega_R^2}{\pi} \frac{\text{Period}}{\tau_D} - \rho_0 k_z^2 \frac{dv_C^2}{dr} \\ &\approx -\rho_0 k_z^2 \frac{dv_C^2}{dr} \end{aligned}$$

since $\tau_D/\text{Period} \ll 1$.

Hence, the result for the perpendicular vorticity is given by

$$(\nabla \times \xi)_\phi \approx ik_z^3 \frac{\pi^2}{\rho_0 \omega_R^4} \frac{v_s^2}{v_A^2 + v_s^2} \frac{dv_C^2}{dr} \left\{ \frac{\tau_D}{\text{Period}} \right\}^2 P'.$$

Next, we will simplify the expression in Eq. (6) for the parallel component of vorticity, $(\nabla \times \xi)_z$. Since there are no terms that contain $\omega^2 - \omega_C^2$, we can again forget about the damping decrement according to Eq. (15) and use

$$\omega^2 \approx \omega_R^2 = \omega_C^2(r_C).$$

From Eq. (19), we have the following:

$$\begin{aligned} \frac{d}{dr} \{\rho_0(\omega^2 - \omega_A^2)\} &= \frac{d\rho_0}{dr} (\omega^2 - \omega_A^2) - \rho_0 k_z^2 \frac{dv_A^2}{dr} \\ &\approx -\frac{d\rho_0}{dr} \frac{v_A^2}{v_s^2} \omega_R^2 - \rho_0 k_z^2 \frac{dv_A^2}{dr}. \end{aligned}$$

Then, from this and Eq. (19), we find

$$\begin{aligned} (\nabla \times \xi)_z &\approx -i \frac{m}{r} \left(\frac{v_s^2}{v_A^2} \right)^2 \frac{1}{\rho_0^2 \omega_R^4} \\ &\cdot \left\{ -\frac{d\rho_0}{dr} \left(\frac{v_A^2}{v_s^2} \right) \omega_R^2 - \rho_0 k_z^2 \frac{dv_A^2}{dr} \right\} P'. \end{aligned} \quad (21)$$

Finally, from Eq. (3), the radial and perpendicular components of the displacement are found to be

$$\begin{aligned} \xi_r &\approx -\frac{1}{\rho_0} \frac{v_s^2}{v_A^2} \frac{1}{\omega_R^2} \frac{dP'}{dr}, \\ \xi_\perp &= \xi_\phi \approx -i \frac{m}{r} \frac{1}{\rho_0} \frac{v_s^2}{v_A^2} \frac{1}{\omega_R^2} P'. \end{aligned} \quad (22)$$

The case of axisymmetric ($m = 0$) slow waves is a bit simpler because some quantities become 0. We note that ξ_ϕ , $(\nabla \times \xi)_r$,

and $(\nabla \times \xi)_z$ are indeed proportional to m and thus vanish for the $m = 0$ modes. On the other hand, the expressions for ξ_r , ξ_z , $\nabla \cdot \xi$, and $(\nabla \times \xi)_\phi$ do not depend explicitly on m . However, they do depend implicitly on m since P' depends on m . In any case, the expressions for axisymmetric modes around the ideal cusp resonant position for the components of the Lagrangian displacement and for the compression are given by

$$\begin{aligned} \xi_r &= -\frac{1}{\rho_0} \frac{v_s^2}{v_A^2} \frac{1}{\omega_R^2} \frac{dP'}{dr}, \\ \xi_\perp &= \xi_\phi = 0, \\ \xi_z &\approx k_z \frac{v_s^2}{v_s^2 + v_A^2} \frac{\pi}{\rho_0 \omega_R^2} \frac{\tau_D}{\text{Period}} P', \\ \nabla \cdot \xi &\approx -i \frac{\pi}{\rho_0 (v_s^2 + v_A^2)} \frac{\tau_D}{\text{Period}} P'. \end{aligned} \quad (23)$$

The components of the vorticity are given by

$$\begin{aligned} (\nabla \times \xi)_r &= 0, \\ (\nabla \times \xi)_\phi &\approx ik_z^3 \frac{\pi^2}{\rho_0 \omega_R^4} \frac{v_s^2}{v_A^2 + v_s^2} \frac{dv_C^2}{dr} \left\{ \frac{\tau_D}{\text{Period}} \right\}^2 P', \\ (\nabla \times \xi)_z &= 0. \end{aligned} \quad (24)$$

The conclusion of this section is that ξ_z , $\nabla \cdot \xi$, and $(\nabla \times \xi)_\phi$ are the dominant quantities and that

$$\xi \approx \xi_z \mathbf{1}_z, \quad \nabla \times \xi \approx (\nabla \times \xi)_\phi \mathbf{1}_\phi. \quad (25)$$

The waves in the cusp continuum are compressive with large parallel motions and carry a huge amount of perpendicular vorticity. This implies that the waves are similar to the slow magnetosonic waves from an infinite homogeneous plasma, although they also have some slight classical Alfvén wave properties since their parallel vorticity is non-zero. The results are in the first order independent of the wave number m .

Goossens et al. (2020) used the approximate analytical expression Eq. (1) for τ_D/Period for the damping in the Alfvén continuum to obtain expressions that depend on the equilibrium quantities ρ_i , ρ_e , l/R , and α and on the wave numbers m and $k_z R$. This has not been done in the present case since the analytical expressions involving τ_D/Period derived in this section are rather involved.

4. Spatial variation for resonant slow (and Alfvén) waves

In this section, we verify our analytical predictions with numerical calculations. The aim is to understand the behaviour of waves in the cusp continuum by looking at the profiles of compression as well as at the displacement and vorticity components. Because of the inclusion of resistivity in the calculations, the quantities that have a pole at the resonant position in ideal MHD will actually be very large, though finite, thanks to dissipation.

A brief description for the resistive solutions is as follows, and we refer interested readers to Chen et al. (2018) and Chen et al. (2020) for more details. We modelled a photospheric waveguide as a static, straight, field-aligned plasma cylinder. The equilibrium quantities depend only on r in such a way

SSKM with $l/R=0.1$ and $kR=0.7$ at $R_m=10^9$

that the equilibrium configuration comprises a uniform interior (denoted by the subscript i) and a uniform exterior (subscript e) as well as a TL continuously connecting the two. In the TL, the squared cusp (v_c^2) and adiabatic sound speeds (v_s^2) were taken to depend on r through $\sin[\pi(r-R)/l]$, where R is the mean waveguide radius and l is the TL width. With pores and sunspot umbrae in mind, we fixed the characteristic speeds [v_{Si} , v_{Se} , v_{Ae}] at $[0.5, 0.75, 0.25]v_{Ai}$. We adopted a rather narrow TL by adopting an l/R of 0.1. Working in the framework of linear, resistive MHD, we then formulated and numerically solved the relevant EVP with the general-purpose finite-element code PDE2D (Sewell 1988). We examined the resonant damping of both SSKMs and SSSMs. This was done by locating the range of sufficiently large magnetic Reynolds numbers (R_m) where the eigenfrequencies depend only on the dimensionless axial wavenumber (kR) but are R_m -independent. We refer to this range of R_m as ‘the resonant regime’. It turns out that the critical R_m , only beyond which the collective modes enter the resonant regime, is somehow dependent on kR . In the figures below, we consistently choose an R_m that is barely inside the resonant regime.

Looking back at Eqs. (3) and (6) for the general expressions of compression as well as displacement and vorticity components, we expect each of these quantities to be non-zero in a uniform plasma, except the parallel vorticity. In a non-uniform plasma, parallel vorticity is also expected to be non-zero. Near the cusp resonant position, the perpendicular component of vorticity is expected to be much larger than its radial and parallel components, and the parallel component of displacement is expected to be much larger than its radial and perpendicular components.

We will first look at the SSKM. Figure 1 shows the total pressure and the three components of the Lagrangian displacement, whereas Figure 2 shows compression and the three components of the vorticity of an SSKM with a frequency ranging in both the Alfvén and cusp continua. The cusp resonant position is close to the left border of the inhomogeneous layer at a position $r/R \approx 0.955$, while the Alfvén resonant position is situated near $r/R \approx 1$.

As can be seen in the two mentioned figures, the parallel displacement (ξ_z), compression ($\nabla \cdot \xi$), radial vorticity ($(\nabla \times \xi)_r$), and perpendicular vorticity ($(\nabla \times \xi)_\theta$) peak at the cusp resonant position. This happens because of the factor (16) in their respective expressions, as is visible in Eqs. (3) and (6), and the fact that P' is constant at the cusp resonant position (Sakurai et al. 1991). However, only the perpendicular vorticity has this factor with $n = 2$; the others have it with $n = 1$. Therefore, perpendicular vorticity is expected to be the most dominant quantity in the cusp resonance; this is confirmed in the figures, which show that perpendicular vorticity has an amplitude three orders of magnitude higher than both the radial vorticity and compression.

At the Alfvén resonant position, parallel vorticity and perpendicular displacement are the dominant quantities as they peak at the Alfvén resonant position. This was already discussed in Goossens et al. (2020) for a pressureless plasma. Radial and perpendicular displacement as well as radial and perpendicular vorticity and compression are then non-zero but definitely smaller than parallel vorticity and perpendicular displacement. It should be noted that the radial displacement jumps at both the cusp and Alfvén resonant positions, while the total pressure is continuous at both positions. This is in accordance with the derivations of Sakurai et al. (1991) in the case of a straight background magnetic field.

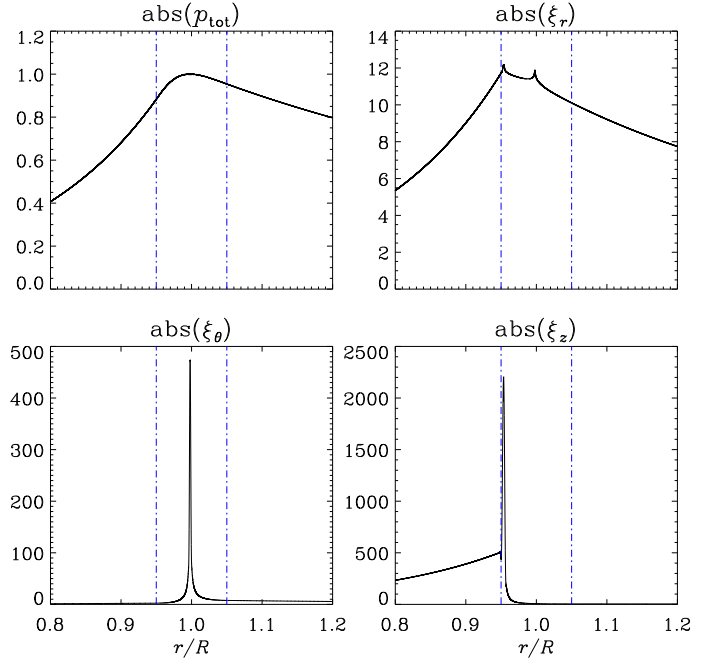


Fig. 1. Modulus of the total pressure (top left), radial displacement (top right), perpendicular displacement (bottom left), and parallel displacement (bottom right) for the slow surface kink ($m = 1$) mode. Here, $l/R = 0.1$, $k_z R = 0.7$, and $R_m = 10^9$ have been taken.

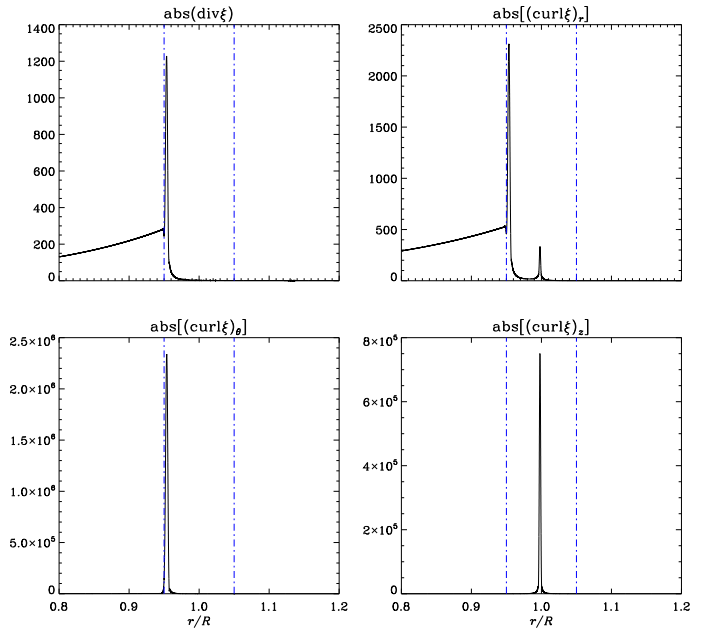
SSKM with $l/R=0.1$ and $kR=0.7$ at $R_m=10^9$


Fig. 2. Modulus of compression (top left), radial vorticity (top right), perpendicular vorticity (bottom left), and parallel vorticity (bottom right) for the slow surface kink ($m = 1$) mode. Here, $l/R = 0.1$, $k_z R = 0.7$, and $R_m = 10^9$ have been taken.

We will now take a look at the particular case of the SSSM (see Figure 3). Since in this case $m = 0$, equations (23) and (24) tell us that the perpendicular component of displacement as well as the radial and parallel components of vorticity are zero everywhere. Figure 3 shows that, again, the compression, perpendicular vorticity, and parallel displacements are the dom-

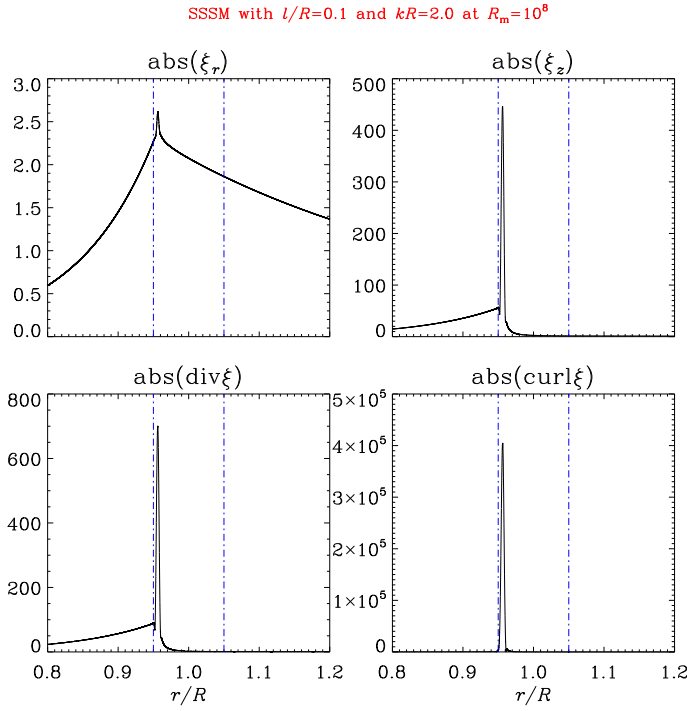


Fig. 3. Modulus of the radial displacement (top left), parallel displacement (top right), compression (bottom left), and perpendicular vorticity (bottom right) for the slow surface sausage ($m = 0$) mode. Here, $l/R = 0.1$, $k_z R = 2$, and $R_m = 10^8$ have been taken.

inant quantities as they peak at the cusp resonant position near $r/R = 0.955$. The perpendicular vorticity is again the most dominant. As pointed out by Sakurai et al. (1991), there is no resonant absorption in the Alfvén continuum for the sausage modes. This explains the absence of a second peak near $r/R = 1$.

The dissipation in the numerical calculation is physical due to magnetic diffusivity η . It is instructive to try to understand the behaviour of the solution in the dissipative layer. The behaviour of the eigenfunctions in the dissipative layer in visco-resistive non-stationary MHD was studied for incompressible plasmas by Ruderman et al. (1995). For incompressible plasmas, the cusp and Alfvén resonances coincide. A simpler mathematical treatment was given by Tirry & Goossens (1996) for compressible plasmas. They treated the Alfvén resonance in detail but did not give expressions for the cusp resonance. Mathematical aspects of the cusp resonance in resistive non-stationary MHD were discussed in, for example, Tirry et al. (1998) and Pintér et al. (2007). A further discussion on the eigenfunctions for the Alfvén resonance can be found in Goossens et al. (2011).

The important quantities in this discussion are δ_A and Λ_A for the Alfvén resonance and δ_C and Λ_C for the slow resonance. Expressions for δ_A and δ_C (the thicknesses of the dissipative layers) are given in Sakurai et al. (1991). When only magnetic diffusivity is taken into account,

$$\delta_A = \left\{ \frac{\omega \eta}{|\Delta_A|} \right\}^{1/3}, \quad \text{and} \quad \delta_C = \left\{ \frac{\omega \eta}{|\Delta_C|} \frac{\omega_C^2}{\omega_A^2} \right\}^{1/3},$$

with

$$\Delta_A = \frac{d}{dr}(\omega^2 - \omega_A^2(r)), \quad \text{and} \quad \Delta_C = \frac{d}{dr}(\omega^2 - \omega_C^2(r)).$$

The expression for Λ_A is given in Tirry & Goossens (1996). The corresponding expression for Λ_C can be found in Tirry et al. (1998) and in Pintér et al. (2007). The Λ_C is formally the same as Λ_A , with the index A replaced by the index C :

$$\Lambda_A = \frac{2\omega_I \omega_A}{\delta_A |\Delta_A|}, \quad \text{and} \quad \Lambda_C = \frac{2\omega_I \omega_C}{\delta_C |\Delta_C|}.$$

From the analysis in Tirry & Goossens (1996), it follows that the change from non-oscillatory behaviour to oscillatory behaviour occurs at about $\Lambda \approx 2$. For the SSKM in Figures 1-2, we used $l/R = 0.1$, $R_m = 10^9$, and $k_z R = 0.7$. The values for Λ_A and Λ_C are then

$$\Lambda_A = 0.029, \quad \text{and} \quad \Lambda_C = 0.41.$$

For the SSKM in Figure 3, we used $l/R = 0.1$, $R_m = 10^8$, and $k_z R = 2$, so that for Λ_C we have

$$\Lambda_C = 0.73.$$

These low Λ_A and Λ_C values confirm that the non-stationary resistive solutions are in the non-oscillatory regime, as can clearly be seen in Figures 1-3.

5. Conclusions

In this paper, we studied the properties of MHD waves undergoing resonant absorption in the cusp continuum in the framework of non-stationary ideal MHD. As discussed by Goossens et al. (2019), MHD waves in an inhomogeneous plasma do not have clearly distinguished properties that would permit one to classify them as Alfvén waves, fast magnetosonic waves, or slow magnetosonic waves, unlike in the case of an infinite homogeneous plasma. For MHD waves in an inhomogeneous plasma, compression, the three vorticity components, and the three displacement components are all non-zero, and hence the waves have a mix of the properties from waves in a homogeneous plasma. We note that the slow and Alfvén resonant waves are driven by the total pressure perturbations P' , as pointed out by Hollweg & Yang (1988).

For waves with a frequency in the cusp continuum, we found that perpendicular vorticity and parallel displacement greatly dominate the other components. Nevertheless, parallel vorticity, though much smaller than perpendicular vorticity, is clearly non-zero in the inhomogeneous layer. These results confirm that the waves have mixed properties, although the waves undergoing resonant absorption in the cusp continuum clearly have properties that closely resemble the properties of the so-called slow waves (i.e. slow magnetosonic waves in a uniform plasma of infinite extent).

For waves with a frequency in the Alfvén continuum, it is the parallel component of vorticity and the perpendicular displacement that greatly dominate the other components of the respective quantities. Nevertheless, these other components and quantities, such as compression, are non-zero as well. This again confirms the mixed properties of the waves, which have properties that are closest to the classical Alfvén waves when undergoing resonant absorption in the Alfvén continuum. This is in line with what was found by Goossens et al. (2020) for waves undergoing resonant absorption in the Alfvén continuum in a pressureless plasma.

Acknowledgements. This research was supported by the National Natural Science Foundation of China (BL: 41674172, 1111761141002, 41974200; SXC:41604145). M.G. was supported by the C1 Grant TRACESpace of Internal Funds KU Leuven (number C14/19/089). TVD was supported by the European Research Council (ERC) under the European Union's Horizon 2020 research and innovation programme (grant agreement No 724326) and the C1 grant TRACESpace of Internal Funds KU Leuven. The research benefitted greatly from discussions at ISSI-BJ.

References

- Arregui, I. & Goossens, M. 2019, A&A, 622, A44
- Chen, S.-X., Li, B., Shi, M., & Yu, H. 2018, ApJ, 868, 5
- Chen, S. X., Li, B., Van Doorselaere, T., Goossens, M., & Geeraerts, M. 2020, ApJ, submitted
- De Pontieu, B., McIntosh, S. W., Carlsson, M., et al. 2007, Science, 318, 1574
- Dorotovič, I., Erdélyi, R., & Karlovský, V. 2008, in IAU Symposium, Vol. 247, Waves & Oscillations in the Solar Atmosphere: Heating and Magneto-Seismology, ed. R. Erdélyi & C. A. Mendoza-Briceno, 351–354
- Fujimura, D. & Tsuneta, S. 2009, ApJ, 702, 1443
- Geeraerts, M., Van Doorselaere, T., Chen, S.-X., & Li, B. 2020, ApJ, 897, 120
- Gilchrist-Millar, C. A., Jess, D. B., Grant, S. D. T., et al. 2020, arXiv e-prints, arXiv:2007.11594
- Goossens, M., Andries, J., & Arregui, I. 2006, Philosophical Transactions of the Royal Society of London Series A, 364, 433
- Goossens, M., Andries, J., & Aschwanden, M. J. 2002, A&A, 394, L39
- Goossens, M., Andries, J., Soler, R., et al. 2012, ApJ, 753, 111
- Goossens, M., Arregui, I., Ballester, J. L., & Wang, T. J. 2008, A&A, 484, 851
- Goossens, M., Arregui, I., Soler, R., & Van Doorselaere, T. 2020, A&A, 641, A106
- Goossens, M., Erdélyi, R., & Ruderman, M. S. 2011, Space Sci. Rev., 158, 289
- Goossens, M., Hollweg, J. V., & Sakurai, T. 1992, Sol. Phys., 138, 233
- Goossens, M., Ruderman, M. S., & Hollweg, J. V. 1995, Sol. Phys., 157, 75
- Goossens, M. L., Arregui, I., & Van Doorselaere, T. 2019, Frontiers in Astronomy and Space Sciences, 6, 20
- Grant, S. D. T., Jess, D. B., Moreels, M. G., et al. 2015, ApJ, 806, 132
- Guo, M., Li, B., & Van Doorselaere, T. 2020, arXiv e-prints, arXiv:2010.06991
- Hasegawa, A. & Uberoi, C. 1982, The Alfvén Wave, DOE critical review Series-Advances in fusion science and engineering (Technical Information Center, U.S. Department of Energy.)
- Hollweg, J. V. 1990, J. Geophys. Res., 95, 2319
- Hollweg, J. V. & Yang, G. 1988, J. Geophys. Res., 93, 5423
- Hood, A. W., Ruderman, M., Pascoe, D. J., et al. 2013, A&A, 551, A39
- Keppens, R. 1995, Sol. Phys., 161, 251
- Keys, P. H., Morton, R. J., Jess, D. B., et al. 2018, The Astrophysical Journal, 857, 28
- Moreels, M. G., Freij, N., Erdélyi, R., Van Doorselaere, T., & Verth, G. 2015, A&A, 579, A73
- Morton, R. J., Verth, G., Jess, D. B., et al. 2012, Nature Communications, 3, 1315
- Parker, E. N. 1991, ApJ, 376, 355
- Pascoe, D. J., Hood, A. W., de Moortel, I., & Wright, A. N. 2012, A&A, 539, A37
- Pascoe, D. J., Wright, A. N., & De Moortel, I. 2010, ApJ, 711, 990
- Pascoe, D. J., Wright, A. N., & De Moortel, I. 2011, ApJ, 731, 73
- Pintér, B., Erdélyi, R., & Goossens, M. 2007, A&A, 466, 377
- Ruderman, M. S. & Roberts, B. 2002, ApJ, 577, 475
- Ruderman, M. S. & Terradas, J. 2013, A&A, 555, A27
- Ruderman, M. S., Tirry, W., & Goossens, M. 1995, Journal of Plasma Physics, 54, 129
- Sakurai, T., Goossens, M., & Hollweg, J. V. 1991, Sol. Phys., 133, 227
- Sewell, G. 1988, The Numerical Solution of Ordinary and Partial Differential Equations (San Diego: Academic Press)
- Soler, R., Goossens, M., Terradas, J., & Oliver, R. 2013, ApJ, 777, 158
- Soler, R., Oliver, R., Ballester, J. L., & Goossens, M. 2009, ApJ, 695, L166
- Tirry, W. J. & Goossens, M. 1995, J. Geophys. Res., 100, 23687
- Tirry, W. J. & Goossens, M. 1996, ApJ, 471, 501
- Tirry, W. J., Goossens, M., Pintér, B., Čadež, V., & Vanlommel, P. 1998, ApJ, 503, 422
- Van Doorselaere, T., Andries, J., Poedts, S., & Goossens, M. 2004, ApJ, 606, 1223
- Verth, G. & Jess, D. B. 2016, Washington DC American Geophysical Union Geophysical Monograph Series, 216, 431
- Yu, D. J. & Van Doorselaere, T. 2019, Physics of Plasmas, 26, 070705
- Yu, D. J., Van Doorselaere, T., & Goossens, M. 2017, A&A, 602, A108